INTERACTIVE CONTROL ENGINEERING
Principles and Applications

Volume 7 Nonlinear Dynamics, Oscillations, and Stabilization

CHAPTER 11

Active Suspension Simulator for Comfort and Road Holding Through One Strut Force

Pages 263–287

Edited by John D. Hedengren

How to cite this chapter. "Active Suspension Simulator for Comfort and Road Holding Through One Strut Force," in *Nonlinear Dynamics, Oscillations, and Stabilization*, John D. Hedengren, Ed., vol. 7 of *Interactive Control Engineering: Principles and Applications*. Advanced Process Solutions, LLC, 2026, ch. 11, pp. 263–287.

The page numbers in this file are those of the printed volume.

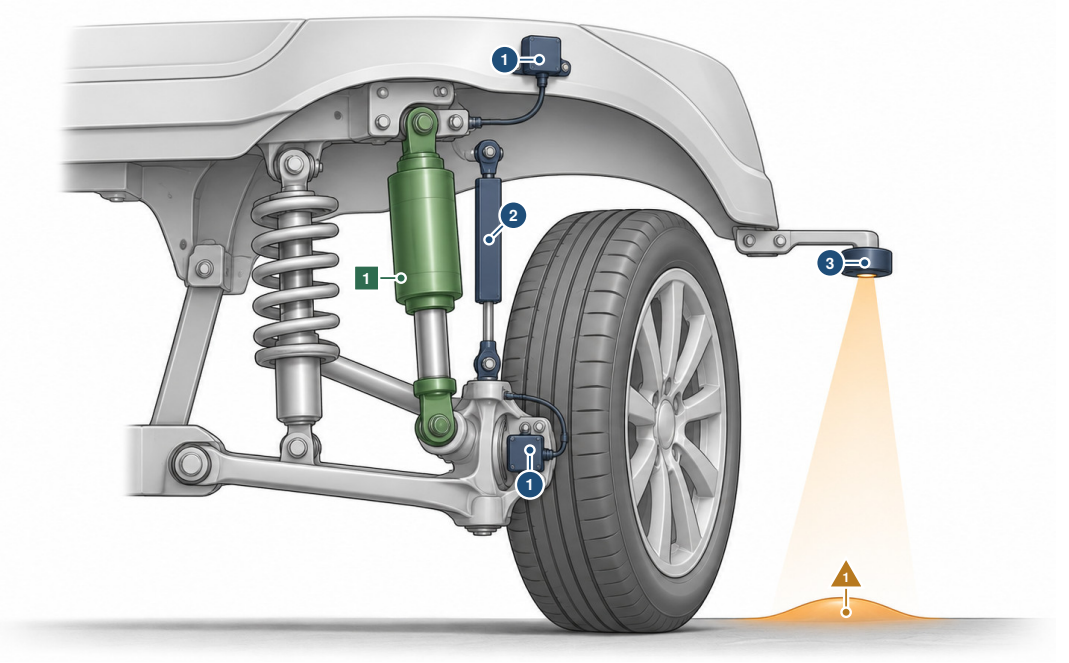
The app for this chapter
https://apmonitor.com/apps/active-suspension/

The volume online: contents, other chapters and citation records
https://apmonitor.com/apps/books/v07-nonlinear-stabilization/#active-suspension

Copyright © 2026 Advanced Process Solutions, LLC. All rights reserved. Produced by Advanced Process Solutions, LLC.

CHAPTER 11

Active Suspension Simulator for Comfort and Road Holding Through One Strut Force



The controller moves 1 the force actuator in the strut, which pushes the body up and the wheel down

The controller reads 1 the accelerometers on the body and on the wheel hub

2 the ride-height sensor across the strut's travel 3 the preview sensor that reads the road ahead of the tire

What disturbs it 1 the bump in the road ahead

Notice that the actuator joins the body to the wheel, so every push it gives one it also gives the other, while the sensor ahead sees the bump before the tire reaches it. Illustration, not to scale.

IN PLAIN TERMS **One Push Between the Body and the Wheel**

The main idea. A car body should stay still for the people inside, while the wheel under it must follow the road to keep its grip. A controlled strut between them can push the body up, but the same push drives the wheel down.

The challenge. At the wheel's own bouncing rhythm, a strut tuned for comfort calms the body mainly by letting the tire leave the road. A tire can only push on the road, and a plain damper can only soak up motion.

Why it matters. A tire in the air cannot brake or steer, so a smooth ride can hide a car that is losing its grip.

THREE WAYS TO READ THIS CHAPTER

Explore	12 min	the first page, the fact in the Introduction (Section 11.1), the two history segments in Section 11.2, the fact and the try-its in Section 11.6, and the key points
Study	50 min	the whole chapter with its three pause points and the twelve exercises at its end
Practice	20 min	the first page, the results (Section 11.6), Technology in Practice (Section 11.7), Limitations (Section 11.8) and the open challenges

The control question One strut force pushes the body up and the wheel down, and near wheel hop the tire nearly fixes the body acceleration. How much comfort can a passive damper, a semi-active damper and a force actuator each buy before the wheel leaves the road or the strut reaches its stop?

Learning objectives

- Derive the constraint no strut force changes, and compute the two modes and two invariant points of the quarter car.
- Convert a road pattern in distance into a frequency and place it against the body mode and wheel hop.
- Explain why a semi-active damper can only dissipate, and how its valve follows a skyhook and groundhook request.
- Compare comfort, tire load, travel and actuator work across the struts, with and without road preview, against a passive twin.
- Explain why load leveling must stay slow and why actuator slew decides road holding at wheel hop.

Prerequisites Sections 1.4.4 (modes and eigenvalues), 1.4.8 (resonance), 1.4.7 (lag and delay), 1.6.2 (velocity-form PID) and 1.6.1 (engine), with 1.6.3 for the predictive force law.

The app https://apmonitor.com/apps/active-suspension/

See also Volume 20, Chapter 12 for preview read from a buffer keyed by travel distance. Volume 20, Chapter 5 for a ride height held through waves with a look-ahead, and Volume 20, Chapter 2 for a vehicle loop whose behavior changes with speed.

11.1 Introduction

A suspension stands between something that must be kept still and something that must be followed. A car body carries passengers who feel its acceleration, while the wheel beneath it must keep its tire pressed on the road, because the grip available for braking and steering rests on the tire load. The quarter car, one body and one wheel joined by a spring and a strut and standing on a tire, is the standard model for weighing passenger discomfort, suspension working space and tire load variation against one another [1, 2]. A controlled strut adds a force between the two masses, and the whole difficulty is that the same force pushes the body up and the wheel down.

The equations of the two masses, added together, lose the strut force entirely. What remains is a constraint that no strut can change. It fixes the body acceleration at one frequency and the suspension deflection at another, so that only one of the three transfer functions of the quarter car can be chosen freely [3]. The first of these frequencies lies close to wheel hop, the resonance of the wheel on its tire, which is 11.9 Hz in the simulator and which a washboard of 1.25 m ripples reaches at 15 m/s. There a strut tuned for comfort leaves the wheel free to bounce, and it lowers the body acceleration mainly by letting the tire leave the road.

The simulator addresses the belief that a better controller improves every measure of a suspension at once, and the habit of judging a suspension by one comfort number. The class of problem is general. A truck cab on its chassis and a railcar body on its bogie each place a suspension force between a payload and an intermediate mass that follows a moving base, and each inherits the same constraint, because the constraint equations of interconnected subsystems do not depend on the nature of the interconnection [3]. The semi-active force generator itself was first proposed for vibration control in general rather than for cars alone [4].

DID YOU KNOW? Semi-Active Damping Well Beyond Cars

A survey of semi-active suspension control lists applications well beyond the car: the cabins of trucks and tractors, seats, trains, washing machines, buildings and bridges, and artificial legs. In each the semi-active device obeys the passivity constraint of the damper in this chapter: it can only dissipate energy [5].

However, the quarter car usually reaches a control course as a linear transfer function, which shows the two modes and hides three facts that decide the outcome on a real road. The tire can push on the road but never pull, a damper can take energy out but never put it in [1], and feedback cannot answer a bump before the wheel reaches it, which is the gap preview control fills [6]. A comfort number read on its own can hide a wheel that spent 1.62 s of 5 s in the air, as case 3 shows.

This chapter establishes how much comfort a passive damper, a semi-active damper and a force actuator can each buy before the wheel leaves the road or the strut reaches its stop. It works with a quarter-car simulator in which all three, driven by one control law, are compared at every instant with a passive twin on the same road. The quarter car, skyhook and groundhook damping, preview feedforward and the invariant points are all established material. The simulator is an eleven-state model that treats contact loss and bump-stop contact as counted events, integrates the passive twin beside the controlled car, keeps the semi-active damper dissipative by construction and reads the road ahead from a noisy buffer indexed by distance. Its passive response agrees with the linear transfer function to within 0.1 % at sixteen speeds. Ten scenarios each change one road, one piece of hardware or one setting.

Section 11.2 reviews suspension control from fixed dampers to road preview. Section 11.3 gives the quarter car, its tire, bump stops and roads, and Section 11.4 derives the constraint that no strut force can change, its two invariant points and the limits a pothole edge sets. Section 11.5 describes the force request, the three struts, the load-leveling loop and, in Section 11.5.7, a predictive force law added beside the original one. Section 11.6 reports the measured scenarios, Section 11.7 the sensors, dampers, actuators and control units of real suspensions, Section 11.8 the limitations and Section 11.9 the conclusions. The exercises of Section 11.10 work through the scenarios.

11.2 Suspension Control From Fixed Dampers to Road Preview

A passive spring and damper fix the compromise between ride and road holding when the car is built, and reviews of road vehicle suspension design start from that compromise [2]. Judging a design needs a model of the road as well as of the car. A road profile is described statistically by a displacement spectral density that falls with wavenumber [7], the form behind the ISO 8608 roughness classes, so that a suspension can be assessed on a random road rather than on a single bump.

The first history box below tells how road preview was proposed for suspensions and then solved as an optimal control problem.

HISTORY Reading the Road Ahead, 1968 and 1976

Preview control, in which the input is sensed before it reaches the plant, was proposed for vehicle suspensions in 1968. That study optimized the trade-off between vibration and the clearance needed for suspension travel on statistically described surfaces. Preview could lower the rms vibration by as much as a factor of sixteen at constant clearance, or the clearance by a factor of 223 at constant vibration [6]. The problem was solved again in 1976 as a discrete optimal control problem, with a controller structure suited to practical use [8]. Optimal linear state feedback for a fully active suspension appeared in the same year, and it needed only the body's absolute velocity and its displacements relative to the axle and the road [9].

A cheaper route than a powered actuator followed in 1974, and its ideal law, a damper from the body to a fixed reference in the sky, is the skyhook term of this simulator, as the second history box on the semi-active damper tells.

Table 11.1 Signals, States and Their Roles

Symbol	Role	Nominal	Range
$\ddot{z}_s$	CV, body acceleration	SP 0	—
x	CV, ride height	SP 0 mm	SP ± 40
F_t	output, tire load	3924 N	≥ 0
F_{req}	MV, strut force request	0 N	$\pm F_{av}$
z_s, $\dot{z}_s$, z_u, $\dot{z}_u$	states, body and wheel	0	—
F_a, c_d	states, actuator, damper	0, 500 N s/m	± 2500, 300–4500
$\tilde{z}_s$, $\dot{\tilde{z}}_s$, $\tilde{z}_u$, $\dot{\tilde{z}}_u$	states, passive twin	0	—
s	state, distance	0 m	≥ 0
v	DV, speed	12 m/s	1–35
m_{load}	DV, load on the corner	60 kg	0–250
$z_r(s)$	DV, road (six choices)	humps	—
σ_p	DV, preview noise (1σ)	0.5 mm	0–30
ε_w	DV, damper wear	0 %	0–90
d	DV, actuator derating	0 %	0–90
F_p	DV, bounce-test push	−800 N, 0.4 s	event
—	DV, bump 4 m ahead	60 mm, 3 m	event

HISTORY A Damper That Only Dissipates, 1974 to 1986

The cheaper route of 1974 was a force generator that responds to general feedback signals from a vibrating system yet needs no servomechanism power supply. In computer simulation it performed comparably to fully active vibration control [4]. A 1986 comparison of passive, active and semi-active cars on the quarter-car model derived the semi-active laws from the active ones. Able only to dissipate energy, the semi-active damper switched off wherever the active system would have supplied energy [1], and the theoretical limitations of active vehicle suspensions were examined in the same year [10]. A later survey calls this saturation of the requested force to what the damper can deliver the clipped approach, and finds it very widespread in semi-active control [5].

Constraint equations derived in 1990 showed that the body acceleration and the suspension deflection of the quarter car each have an invariant point within the frequency range of interest, that all three measures can be improved together only near the unsprung natural frequency, and that severe trade-offs exist at every other frequency [3]. Road holding gained a semi-active law of its own when the ground-hook concept, a damper from the wheel to the road, was extended for truck suspensions in 1997 [11], and magnetorheological fluid devices offered another way to vary damping electrically [12]. Linear-quadratic studies clarified the performance potential, the bandwidth requirements and the optimal structure of advanced suspensions, and practical developments followed [13].

Semi-active control laws were later compared on a common single-corner model [5], preview controllers for an active suspension were designed and implemented on a vehicle [14], and a 2015 survey reviewed the state of the art in active and semi-active suspension control [15]. The comfort side of the problem rests on how people perceive vibration in a vehicle [16], which is why a comfort number in this simulator is always read beside a tire load and a travel.

11.3 Quarter Car on a Road Defined in Distance

One corner of a car is simulated in vertical motion only: the quarter body and its load, the wheel with its hub and brake, a spring and a strut unit between them, a tire below and bump stops at the ends of the travel. The car drives at speed v along a road whose height $z_r(s)$ depends on the distance s, so a feature of wavelength λ arrives at the frequency $f = v/\lambda$. Each symbol of the equations is placed on the car in Figure 11.1.

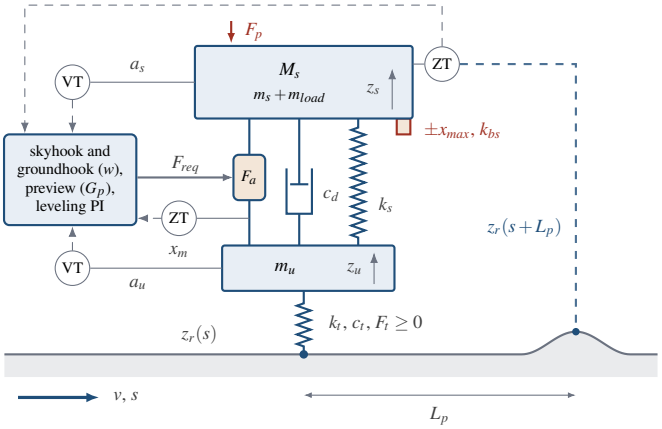


Figure 11.1 One corner of a car as simulated. The body M_s, the quarter body m_s plus the load m_{load}, and the wheel m_u are measured upward from rest at the design load as z_s and z_u, and are joined by the spring k_s and the strut unit, a damper c_d beside an actuator F_a, with bump stops k_{bs} beyond $\pm x_{max}$ of the ride height $x = z_s - z_u$. The tire k_t, c_t pushes on the road $z_r(s)$ and cannot pull, and F_p is the push of the bounce test. Two accelerometers VT and a ride-height sensor ZT reach the controller through noise and a common delay, and the preview sensor ZT reads the road L_p ahead of the wheel. The request F_{req} becomes an actuator force command or a damper valve command. The passive twin, not drawn, is the same car with the fixed damper c_p on the same road.

The signals are classified in Table 11.1. Eleven states are integrated: the body and wheel heights and velocities, the actuator force F_a, the damper coefficient c_d, the four motion states of a passive twin and the distance s. The tire load, the bump-stop force and every event are computed from them after each step.

11.3.1 Body, Wheel and Strut Unit

Heights are measured upward from where the body and the wheel rest on a level road with the design load m_{ref} aboard, and the spring and tire preloads $F_{s0} = (m_s + m_{ref})g$ and $F_{t0} = (m_s + m_{ref} + m_u)g$ hold the car there. The body mass is $M_s = m_s + m_{load}$, so a heavier load settles the body lower until the spring takes it. The two masses obey Equation (11.1).

$$\begin{aligned} M_s\ddot{z}_s &= F_{s0} - k_s x + F_u + F_{bs} + F_p - M_s g \\ m_u\ddot{z}_u &= F_t - F_{s0} + k_s x - F_u - F_{bs} - m_u g \end{aligned} \tag{11.1}$$

where $x = z_s - z_u$ is the ride height measured from the design height, F_u the force of the strut unit, F_{bs} the bump-stop force and F_p the bounce-test push, −800 N for 0.4 s of simulated time when the student presses the body down. A positive F_u pushes the body up and the wheel down by the same amount.

The strut unit is a damper beside an actuator, and both have dynamics of their own, Equation (11.2).

$$\begin{aligned} F_u &= F_a - \eta\, c_d\,(\dot{z}_s - \dot{z}_u) \\ \tau_d\dot{c}_d = c_{cmd} - c_d, &\qquad \tau_a\dot{F}_a = F_{cmd} - F_a \end{aligned} \tag{11.2}$$

where $\eta = 1 - \varepsilon_w/100$ is the fraction of damping left after the wear ε_w in percent, $\tau_d = 15$ ms is the valve lag and $\tau_a = 10$ ms the actuator lag. The passive strut commands $c_{cmd} = c_p = 1800$ N s/m and $F_{cmd} = 0$. The semi-active strut commands c_{cmd} within $[c_{min}, c_{max}] = [300, 4500]$ N s/m and $F_{cmd} = 0$. The active strut commands a force within $\pm F_{av}$ and keeps a residual damper $c_{cmd} = c_{res} = 500$ N s/m that does not wear ($\eta = 1$). A lag of a command that stays inside $[c_{min}, c_{max}]$ stays inside it, so the

damper term is $-\eta c_d(\dot{z}_s - \dot{z}_u)$ with $c_d > 0$ at every instant, including the intermediate stages of the integrator, and the damper can never feed energy in.

11.3.2 Tire, Bump Stops and Events

The tire is a spring and a light damper that can push on the road but not pull, Equation (11.3).

$$F_t = \begin{cases} \max\left(0,\ k_t\delta + c_t\dot{\delta}\right), & \delta > 0 \\ 0, & \delta \le 0 \end{cases} \qquad \delta = F_{t0}/k_t + z_r(s) - z_u \tag{11.3}$$

where δ is the true compression, 19.6 mm at rest, and $\dot{\delta} = v\,z_r'(s) - \dot{z}_u$. Beyond the free travel the bump stops take over, Equation (11.4).

$$F_{bs} = \begin{cases} k_{bs}(-x_{max} - x), & x < -x_{max} \\ -k_{bs}(x - x_{max}), & x > x_{max} \\ 0, & \text{otherwise} \end{cases} \tag{11.4}$$

with $x_{max} = 80\,\text{mm}$ and $k_{bs} = 300\,\text{kN/m}$, twelve times the spring rate. Both nonlinearities enter the right-hand side as force laws, never as clipped coordinates, and both are counted as events. After every step the model checks whether F_t has reached zero or F_{bs} has become nonzero, counts each new liftoff and each new contact, accumulates the time the wheel spends in the air, and marks the place on the road.

11.3.3 Roads

Every road is a function of distance. Humps, potholes and the washboard start 20 m in and the rough road ramps in from 15 m, so each run begins on level road, for 1.67 s over the humps at 12 m/s. A hump of height H and length L, a pothole of depth D and length L_h with rounded edges of length e, and a washboard of amplitude A and wavelength λ follow Equation (11.5).

$$\begin{aligned} z_{hump} &= \tfrac{H}{2}\left[1 - \cos(2\pi u/L)\right], \quad 0 \le u \le L \\ z_{hole} &= -\tfrac{D}{2}\left[1 - \cos(\pi u/e)\right], \quad 0 \le u < e \\ z_{wash} &= A\,r(s)\sin[2\pi(s-20)/\lambda] \end{aligned} \tag{11.5}$$

where $u = (s - 20) \bmod 40$ repeats the hump and the pothole every 40 m, the pothole bottom is flat at $-D$ and its far edge mirrors the near one, $e = \min(0.15\,\text{m}, L_h/2)$ is the width a tire envelops, and $r(s)$ is a raised-cosine ramp over the first 2λ. The defaults are $H = 60\,\text{mm}$, $L = 3\,\text{m}$, $D = 50\,\text{mm}$, $L_h = 0.9\,\text{m}$, $A = 7\,\text{mm}$ and $\lambda = 1.25\,\text{m}$. The rough road is a first-order random process in distance, Equation (11.6).

$$\begin{aligned} z_k &= a z_{k-1} + \sigma\sqrt{1 - a^2}\,\xi_k \\ a &= \mathrm{e}^{-2\pi n_c \Delta s}, \qquad \sigma^2 = \frac{\pi G_{ref}\, n_0^2}{2 n_c} \end{aligned} \tag{11.6}$$

with ξ_k standard normal, $\Delta s = 0.05\,\text{m}$, $n_0 = 0.1$ and $n_c = 0.05$ cycles/m and $G_{ref} = 64 \times 10^{-6}\,\text{m}^3$. Its one-sided spectral density falls as n^{-2} above n_c, and the table is scaled at lookup by $\sqrt{G_d(n_0)/G_{ref}}$, so the ISO 8608 roughness $G_d(n_0) = 256 \times 10^{-6}\,\text{m}^3$, the class C geometric mean, gives a process standard deviation of 8.97 mm. The table holds 1000 m, is blended over its last 20 m into its first point, has its mean removed, is interpolated linearly and is drawn afresh from the seeded generator at every reset. The challenge route joins 100 m of rough road from 15 to 115 m, washboard from 120 to 132 m, each ramped in and out over 5 m and 2λ, a smooth dip 40 mm deep and 2.5 m long at 150 m and a hump at 165 m, and it ends at 185 m. A “Bump ahead” event places a hump of the configured size 4 m in front of the wheel on any road.

11.3.4 Passive Twin, Metrics and Numerics

The passive twin obeys Equations (11.1), (11.3) and (11.4) with states $\tilde{z}_s$, $\tilde{z}_u$ and the unworn damper $F_u = -c_p(\dot{\tilde{z}}_s - \dot{\tilde{z}}_u)$, and it shares the road, the speed, the load and the push. Both cars keep separate metrics, accumulated at every physics step from the reset and frozen when the challenge route ends, Equation (11.7).

$$a_{rms} = \sqrt{\frac{1}{T}\int_0^T \ddot{z}_s^2\,dt}$$
$$\Delta F_{t,rms} = \frac{100}{F_{st}}\sqrt{\frac{1}{T}\int_0^T (F_t - F_{st})^2 dt} \tag{11.7}$$

where $F_{st} = (M_s + m_u)g$ is the static tire load, 3924 N at the design load. Comfort against the twin is $100(a_{rms}/\tilde{a}_{rms} - 1)$ in percent. The scorecard also reports the peak travel $\max|x|$, the liftoffs and the time in the air, the bump-stop hits, the positive mechanical work of the actuator $\int \max[0, F_a(\dot{z}_s - \dot{z}_u)]\,dt$ or the heat taken out by a damper, and the ride time. Comfort is unweighted, and the passenger drawn in the scene takes words adapted from the ISO 2631-1 comfort bands at fixed cut points of a running 1 s rms, as an indication only.

The car starts at rest in its static position on level road, which is the origin at the design load, with c_d at the resting value of the chosen strut and, for an active strut in automatic, F_a holding any load difference from m_{ref} at the ride height setpoint. The engine of Section 1.6.1 advances the states by the fourth-order Runge-Kutta method on a fixed 0.5 ms step, the controller runs every 2 ms, and the historian logs 100 samples per second. The equilibrium residual at the design load is 2.1×10^{-14}, and halving the step changes the rms, the peak and the tire-load rms of case 1 over 5 s by a relative 1.6×10^{-5}, both from the application's own tests. The noise generator is seeded with 20261013 (20261014 for case 8 and 20261015 for the challenge), so every run replays exactly.

The parameters and the default settings are listed in Table 11.2. The simulation runs at 0.1, 0.25, 0.5, 1 and 2 times real time, 0.5 by default, and the trends offer windows of 2, 6, 15 and 30 s.

11.3.5 Assumptions

The car is one corner in vertical motion. Pitch, roll and the load transfer from the other wheels are absent and the passenger moves rigidly with the body without a seat, which breaks down in braking and cornering and for any control of pitch and roll.

The spring and the tire are linear, the bump stops are stiff linear one-sided springs and the strut has no friction. The tire touches the road at one point and follows the profile exactly except at the pothole edges, which are rounded to the width a tire envelops. The idealization breaks down for features shorter than the contact patch, which a real tire bridges, and for edges it flattens.

The road is a single rigid track and the speed is constant between changes. Longitudinal and lateral tire forces are not modeled, so grip is represented by the vertical tire load alone, the quantity the braking and steering forces scale with, and the model does not hold during hard braking.

The actuator is a first-order lag with a slew limit and a force limit, which leaves out valve and pressure dynamics. Its energy counts positive mechanical work only, with no electrical or hydraulic losses, no regeneration and no power for holding a static force, which a real hydraulic unit does spend.

The sensors carry white noise and one common delay, and the preview reading is the true profile plus independent noise, which a camera's biased errors would violate. The speed and the distance are known exactly. Comfort is the unweighted rms body acceleration, a comparison between struts on the same road rather than a rating in the sense of ISO 2631-1.

Table 11.2 Parameters, Adjustable in the Model Panel Unless Marked Hidden, and Default Settings of the Control Cards Below the Rule

Symbol	Meaning	Value	Range
m_s	quarter body, empty	300 kg	200–500
m_{ref}	design load	60 kg	0–200
m_u	wheel, hub and brake	40 kg	25–80
k_s	suspension spring	25 kN/m	10–60
k_t, c_t	tire stiffness, damping	200 kN/m, 100 N s/m	100–350, 0–1000
x_{max}, k_{bs}	free travel, bump stop	80 mm, 300 kN/m	40–150, 50–1000
g	gravity (hidden)	9.81 m/s^2	9.7–9.9
c_p	passive damper	1800 N s/m	300–6000
c_{min}, c_{max}	semi-active range	300, 4500 N s/m	100–1500, 1500–9000
τ_d	damper valve lag	15 ms	2–80
c_{res}	residual damper, active	500 N s/m	0–3000
F_{max}	actuator force limit	2500 N	300–6000
$\dot{F}_{max}$	actuator slew limit	400 kN/s	20–1000
τ_a	actuator lag	10 ms	2–100
t_d	sensor delay	2 ms	0–50
σ_{as}, σ_{au}	accelerometer noise	0.02, 0.2 m/s^2	0–0.5, 0–3
σ_x	ride-height noise	0.5 mm	0–5
τ_v, τ_h	velocity leak, height filter	1.0, 1.0 s	0.2–5, 0.1–5
L_p, t_{lead}	preview distance, lead	5 m, 20 ms	1–15, 0–100
H, L	hump height, length	60 mm, 3 m	10–120, 0.5–6
D, L_h	pothole depth, length	50 mm, 0.9 m	10–120, 0.4–3
A, λ	washboard	7 mm, 1.25 m	2–30, 0.3–6
$G_d(n_0)$	roughness	256×10^{-6} m^3	16–1024 (10^{-6})
—	feature spacing (hidden)	40 m	20–100
w	comfort preference	70 %	0–100
C_{sky}, C_{gnd}	skyhook, groundhook gains	4000, 2500 N s/m	0–10000
K_c, τ_I	leveling gain, integral time	5 N/mm, 0.5 s	0–50, 0.1–20
h_{SP}	ride height setpoint	0 mm	−40–40
G_p, W	preview gain, window	1, 0.3 m	0–1.5, 0.05–2

11.4 One Force on Two Masses

11.4.1 Modes and the Constraint

At the design load the body bounces on the spring and tire in series at $\sqrt{k_s k_t/[(k_s+k_t)M_s]}/2\pi = 1.25$ Hz, and the wheel hops between the spring and the tire at $\sqrt{(k_s+k_t)/m_u}/2\pi = 11.94$ Hz. The coupled undamped frequencies are 1.2496 and 11.945 Hz, so the two approximations the application displays are within 0.1 %. With the damper at c_p the eigenvalues of the linear car (Section 1.4.4) give damping ratios of 0.25 for the body mode and 0.33 for wheel hop.

Adding the two lines of Equation (11.1) removes the spring, the strut and the bump stops. With the tire on the road and the load at its design value, what is left is Equation (11.8).

$$M_s\ddot{z}_s + m_u\ddot{z}_u = k_t(z_r - z_u) + c_t(\dot{z}_r - \dot{z}_u) + F_p \tag{11.8}$$

Apart from the push of the bounce test, only the tire can change the total momentum of the corner. Whatever the strut does for one mass it undoes for the other, and the controller chooses only how the tire force is shared between them.

11.4.2 Two Invariant Points

For a harmonic road $z_r = Z_r e^{j\omega t}$, and with c_t neglected, Equation (11.8) gives the two relations of Equation (11.9).

$$\begin{aligned} -\omega^2 M_s Z_s &= k_t Z_r - (k_t - \omega^2 m_u) Z_u \\ k_t(Z_r - Z_u) &= -\omega^2 \left[(M_s + m_u)Z_u + M_s X\right] \end{aligned} \tag{11.9}$$

where $X = Z_s - Z_u$ is the amplitude of the ride height. At $\omega_1 = \sqrt{k_t/m_u}$ the wheel drops out of the first line, and the body acceleration is $k_t Z_r/M_s$ whatever the strut does. At $\omega_2 = \sqrt{k_t/(M_s+m_u)}$ the

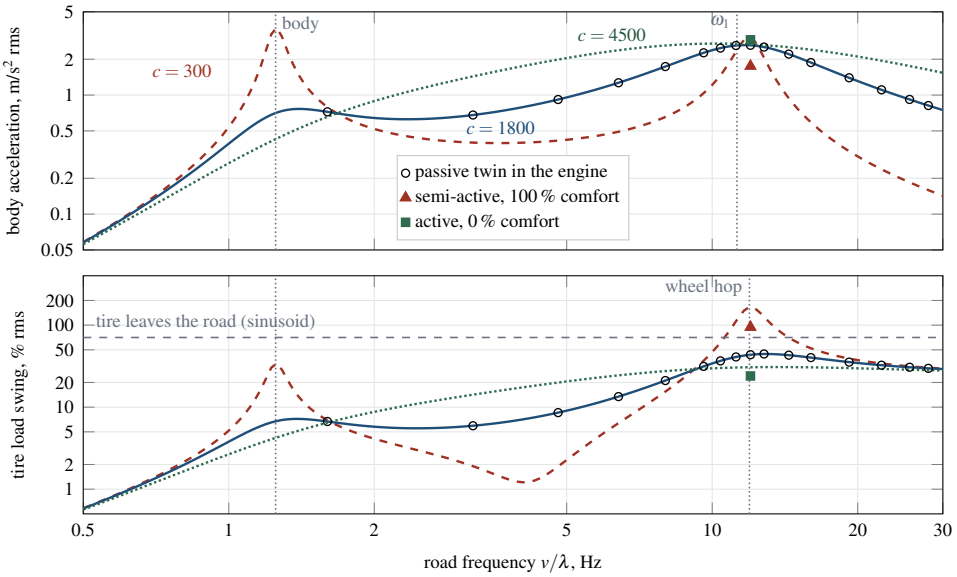


Figure 11.2 Steady response of the quarter car to the 7 mm washboard against road frequency. The lines are the linear model with a damper of 300 (dashed), 1800 (solid) or 4500 N s/m (densely dotted), the circles the passive twin in the running engine at 2 to 35 m/s, and the filled triangle and square the semi-active strut at 100 % comfort (case 3) and the active strut at 0 % with its full force (case 7 before the derating), both at 15 m/s. The dotted lines mark the body mode, the invariant point ω_1 and wheel hop, and above the horizontal dashed line a sinusoidal tire load would reach zero.

wheel drops out of the second, and the ride height is $X = -(M_s + m_u)Z_r/M_s$. These are the invariant points of the quarter car [3]. For the default car $\omega_1/2\pi = 11.25$ Hz, just below wheel hop, where the body acceleration is 0.556 m/s^2 per millimeter of road, and $\omega_2/2\pi = 3.56$ Hz, where the travel is 1.11 times the road amplitude. The tire damping of 100 N s/m blurs the first point slightly, so passive dampers from 300 to 4500 N s/m give 0.483 to 0.544 m/s^2 per millimeter there.

Both relations hold only while $F_t > 0$, because Equation (11.3) is linear only in contact. A strut can therefore lower the body acceleration at wheel hop by more than the blur only by unloading the tire until it leaves the road. In the linear model, a pure skyhook law of 4000 N s/m with the residual damper brings the washboard response at 11.25 Hz from 2.61 to 2.39 m/s^2 rms but needs a tire-load swing of 94.2 % rms, an amplitude of 133 % of the static load, which a tire that cannot pull does not have. A lag-free version of the default blend gains 2 %, 2.56 against 2.61 m/s^2, and raises the tire-load swing from 41.1 to 52.8 %.

🕮 **Pause.** Try Exercise 11.1 before reading on.

11.4.3 Frequency Is Speed Over Wavelength

Because the road is a pattern in distance, the speed decides which mode a road excites. The steady response of the linear passive car to the 7 mm washboard is drawn against $f = v/\lambda$ in Figure 11.2 for the softest, the nominal and the firmest damper. The circles are the passive twin in the running engine at sixteen speeds from 2 to 35 m/s, measured over 5 s once the washboard is fully under the wheel. They agree with the linear curve to within 0.08 % in body acceleration and in tire load, because the passive car is linear while its tire stays down and its travel stays inside the stops, which it does at every one of these speeds. The largest difference is at 2 m/s, where the start-up transient of the body mode has not quite died out.

Three features of Figure 11.2 organize the scenarios. The body acceleration peaks near wheel hop, not near the body mode, because the road input is a displacement and its acceleration grows with the square of the frequency, so the passive twin sees 0.92 m/s^2 rms at 6 m/s, 2.62 m/s^2 at 15 m/s and 1.11 m/s^2 at 28 m/s. The three dampers nearly meet at ω_1 and separate on either side, soft damping calming the body away from the two resonances and firm damping calming it at them. The soft damper's tire load crosses the liftoff line around wheel hop, which is where the comfort-biased struts of case 3 lose the road.

11.4.4 What No Strut Can Follow

A steep pothole edge asks more of the wheel than any strut can supply. Following the entry edge of Equation (11.5) needs a downward acceleration of $(D/2)(\pi v/e)^2$, which is 1579 m/s^2 at 12 m/s. Once the tire unloads, the spring preload and the wheel's own weight accelerate it downward at most at $(F_{s0}+m_u g)/m_u = 98.1\,\mathrm{m/s^2}$, less whatever the damper resists, and a fully pushing actuator adds $F_{max}/m_u = 62.5\,\mathrm{m/s^2}$. The wheel can follow the edge only below 2.99 m/s, or 3.83 m/s with the whole actuator pushing it down, and at 12 m/s every strut leaves the road. The edge speed, not the controller, decides what happens next.

The semi-active strut has the opposite limit. Its damper force times the relative velocity is $-\eta c_d(\dot z_s-\dot z_u)^2 \le 0$ at every instant, so it can oppose motion with any force its valve range allows and can never assist it. A shipped test finds the largest value of that product over 8 s on the washboard to be -6.6×10^{-36} W, so it never turns positive.

11.5 The Force Request and Its Three Struts

One control law serves every strut, and the hardware decides how much of it is delivered. The controller executes every $\Delta t_c = 2\,\mathrm{ms}$, a 500 Hz loop, before each fourth physics step, and holds its commands over the next 2 ms. It never sees the true state.

11.5.1 Instruments and Estimates

Each scan reads a body accelerometer, a wheel accelerometer and a ride-height sensor, adds white noise of $\sigma_{as} = 0.02\,\mathrm{m/s^2}$, $\sigma_{au} = 0.2\,\mathrm{m/s^2}$ and $\sigma_x = 0.5\,\mathrm{mm}$, and passes all three through one delay line of $t_d = 2\,\mathrm{ms}$ with linear interpolation. Velocities come from leaky integrators and the ride height from a first-order filter, Equation (11.10).

$$\begin{aligned} \hat{\dot z}_{s,k} &= \hat{\dot z}_{s,k-1} + \left(a_{s,m} - \hat{\dot z}_{s,k-1}/\tau_v\right)\Delta t_c \\ \hat x_k &= \hat x_{k-1}\,\mathrm{e}^{-\Delta t_c/\tau_h} + x_m\left(1-\mathrm{e}^{-\Delta t_c/\tau_h}\right) \end{aligned} \tag{11.10}$$

with the same integrator for $\hat{\dot z}_u$ from $a_{u,m}$, $\tau_v = 1\,\mathrm{s}$ and $\tau_h = 1\,\mathrm{s}$. The leak keeps the integrated noise from drifting, attenuates motion below about 0.16 Hz and adds 7° of phase lead at the body mode. The preview sensor reads the road $L_p = 5\,\mathrm{m}$ ahead of the wheel on every scan, adds noise of standard deviation σ_p, and stores the reading against the distance at which it was taken. When the wheel approaches that distance, the controller fits a least-squares line through the stored readings within $\pm W/2$ of the point $q = s + v t_{lead}$, which is where the wheel will be one lead time $t_{lead} = 20\,\mathrm{ms}$ later, and takes its height $\hat z_r$ and slope $\hat z_r'$. With fewer than three readings in the window it interpolates between the two that bracket q. Volume 20, Chapter 12 reads a seam from a buffer indexed by travel distance in the same way, because there too the sensor and the actuator are separated by distance rather than time.

11.5.2 Skyhook, Groundhook and Preview

The request is the sum of three terms, Equation (11.11).

$$\begin{aligned} F_{sky} &= -w C_{sky} \hat{\dot{z}}_s, \qquad F_{gnd} = (1-w) C_{gnd} \hat{\dot{z}}_u \\ F_{prev} &= -G_p \left(k_s \hat{z}_r + c_\pi v \hat{z}_r' \right) \\ F_{dyn} &= F_{sky} + F_{gnd} + F_{prev} \end{aligned} \tag{11.11}$$

where w is the comfort preference, from 0 for pure groundhook to 1 for pure skyhook, and c_π is the passive damping the strut keeps, c_{res} for the active strut and c_{min} for the semi-active one. The skyhook term is a damper from the body to the sky and pulls a rising body down, the groundhook term is a damper from the wheel to the road and pushes a rising wheel down, and a shipped test checks both signs. The preview term cancels what the road under the wheel is about to push through the spring and the damper, so the strut shortens over a hump and lengthens into a dip while the body stays level. It is off by default.

11.5.3 Passive, Semi-Active and Active Hardware

The passive strut ignores the request. The semi-active strut clips it to the rating $\pm F_{max}$, because a damper has no actuator to derate, and sets its valve to produce it where a damper can, Equation (11.12).

$$c_{cmd} = \begin{cases} \text{clip}_{[c_{min},\, c_{max}]} \left(-F_{req} / \hat{v}_{rel} \right), & F_{req} \hat{v}_{rel} < 0 \\ c_{min}, & \text{else} \end{cases} \tag{11.12}$$

with $\hat{v}_{rel} = \hat{\dot{z}}_s - \hat{\dot{z}}_u$ and the first case taken only when $|\hat{v}_{rel}| > 10^{-4}\,\text{m/s}$. When the request has the sign that would feed energy in, the valve goes soft and the delivered force parts from the requested one on the force trend. The strut counts as saturated whenever $|F_{req}| > 25\,\text{N}$ and the damper cannot deliver it.

Pause. Try Exercise 11.2 before reading on.

The active strut delivers the request through its lag and limits, and it alone carries a load-leveling loop, because a damper at rest carries no load. The available force is $F_{av} = F_{max}(1 - d/100)$, and when a derating lowers it the held output drops to the new limit at once rather than slewing down.

11.5.4 Load-Leveling PI in Velocity Form

The leveling loop is the framework's shared PID in its velocity, or incremental, form, with the dynamic request entering as the output bias, Equation (11.13).

$$\begin{aligned} e_k &= h_{SP} - \hat{x}_k, \qquad P_k = K_c e_k \\ S_k &= S_{k-1} + (P_k - P_{k-1}) \\ u_k &= F_{dyn,k} + S_k + I_{k-1} \\ \bar{u}_k &= \text{clamp}(u_k, -F_{av}, F_{av}) \\ F_{cmd,k} &= \text{slew}\left(\bar{u}_k,\ F_{cmd,k-1},\ \dot{F}_{max} \Delta t_c \right) \\ I_k &= I_{k-1} + \left[\frac{K_c}{\tau_I} e_k + \frac{F_{cmd,k} - u_k}{T_t} \right] \Delta t_c \end{aligned} \tag{11.13}$$

The terms are those of Equations (1.12) to (1.15) in Section 1.6.2, with the derivative time zero and the dynamic request as the bias, so the running sum S_k telescopes to $K_c e_k$ and is never clamped. Back-calculation with the tracking time $T_t = \tau_I = 0.5\,\text{s}$ acts on the integral only, and the clamp and the slew limit of 400 kN/s act on the emitted command. The integral line runs only while $K_c/\tau_I \neq 0$, so a leveling gain of zero freezes the integral, and case 5 switches the leveling off by setting $K_c = 0$ before the run, which leaves the integral at its seed of 0 N. Because the fast terms enter as the bias, clipping of the whole request also reaches the leveling integral through the back-calculation. The

Table 11.3 Scenario Sequence

#	Scenario	Setting	Teaching point
1	Isolated bump	12 m/s, active	feedback and preview
2	Pothole	12 m/s, active	contact loss
3	Washboard road	15 m/s, semi, 100 %	wheel hop by tuning
4	Higher speed	passive, 6 to 15 m/s	wheel hop by speed
5	Heavier passenger load	+140 kg at 0.2 s	leveling and travel
6	Reduced damping	passive, 60 % worn	a quiet fault
7	Actuator saturation	0 %, 500 N at 4 s	lost authority
8	Noisy preview	rough, 25 mm at 8 s	trusting a sensor
9	A force plan inside the camera horizon	active, MPC, preview	force and contact
10	Challenge, three surfaces	route, 100 %, no preview	graded run

loop is reverse acting, because a positive force raises the ride height, so the command falls as the measured height rises, and a shipped test checks that a sagging body receives more force. The reset seeds the integral with the resting actuator force, and on a passive or semi-active strut the loop tracks with zero contribution, so switching to the active strut starts it without a jump.

11.5.5 Why the Leveling Is Slow and the Actuator Fast

The defaults are $K_c = 5\,\mathrm{N/mm}$ and $\tau_I = 0.5\,\mathrm{s}$, an integral-dominant loop behind a 1 s height filter. At the body frequency ω_b the filter lags the height by nearly 90°, which turns a proportional term into a force in phase with the body velocity, a negative damping of about $K_c/(\omega_b^2 \tau_h)$. That is 81 N s/m at the default gain and 811 N s/m at the slider's maximum of 50 N/mm. At 70 % comfort the skyhook term dominates and the body stays stable at every gain the slider allows. At 0 % comfort the groundhook's reaction on the body cancels most of the residual damper. A push test on level road with the sensor noise switched off gives the body mode a damping ratio of 0.070 with the residual damper alone, 0.026 once the groundhook term is added, and 0.015 with the leveling at its default gain. Over 40 s the body still decays at 11 N/mm, grows slowly at 12 N/mm, and from 13 N/mm rings into its bump stops.

🕮 **Pause.** Try Exercise 11.3 before reading on.

The actuator is sized for wheel hop. A 400 kN/s slew limit lets it follow a full 2500 N sinusoid up to $\dot{F}_{max}/(2\pi F_{max}) = 25.5\,\mathrm{Hz}$, and its 10 ms lag costs 37° of phase at 11.9 Hz. On the washboard at 15 m/s and 0 % comfort the default actuator holds the tire-load swing to 24.0 % rms with no liftoff. With a 20 ms lag alone it holds 26.7 %, while a slew limit of 50 kN/s alone lets the groundhook force arrive late and pump the wheel, to 97.7 % rms and 60 liftoffs in 5 s. The slew rate, not the lag, decides whether the road-holding law works at wheel hop.

11.5.6 Manual Mode and Model Boundaries

In manual mode the student moves the actuator force of the active strut within $\pm F_{av}$, through the same slew limit, or the valve setting of the semi-active strut within $[c_{min}, c_{max}]$. The leveling integral tracks the manual force, so the return to automatic is bumpless, as a framework test confirms (Section 1.6.2). The simulation model is Equations (11.1) to (11.6). The original controller's internal model is limited to k_s and c_π in the preview term, since the skyhook and groundhook laws need no model, and no model is identified. The linear transfer functions of Section 11.4 are an analysis model of the passive car in contact and are not evaluated by the original control law.

11.5.7 A Nominal Preview Force Optimization

The app also offers a predictive force law, selected as MPC under Active law in place of skyhook and preview. It follows the predictive control option of Section 1.6.3, and this subsection gives

Table 11.4 Measured Results. Values in Parentheses Are the Passive Twin on the Same Road at the Same Instant

#	Configuration and window	Body acceleration	Tire load swing	Travel, events and other
1	70 %, first hump	peak 4.72 (5.90) m/s^2	—	rise 36.7 (47.7) mm, undershoot 5.3 (20.8) mm
1	100 %, first hump	peak 3.09 m/s^2	—	rise 28.4 mm
1	70 % with preview, first hump	peak 1.92 m/s^2	—	rise 5.9 mm, strut compressed 61.1 mm
1	0–10 s: 70 %, 100 %, preview	0.885, 0.596, 0.345 (1.197) rms	8.1, 5.7, 4.3 (11.0) %	actuator work 1, 30, 138 J
2	12 m/s, first pothole	peak 11.45 (13.65) m/s^2	—	2 liftoffs, 42.0 ms (1, 29.0 ms)
2	12 m/s with preview	peak 9.73 m/s^2	—	2 liftoffs, 32.0 ms
2	3 m/s, without and with preview	—	—	12.0 ms (19.5 ms), then none
3	semi-active, 100 %, 3–8 s	1.75 (2.62) rms	94.4 (43.6) %	60 liftoffs, 1.62 s airborne, valve $\leq$ 840 N s/m
3	semi-active, 50 % and 0 %	2.60, 2.64 rms	54.0, 37.5 %	no liftoff, lowest tire load 898 N at 50 %
3	active, 70 %	2.91 rms	52.6 %	no liftoff
4	passive, 6, 15, 28 m/s	0.92, 2.62, 1.11 rms	8.6, 43.6, 32.5 %	road at 4.8, 12.0, 22.4 Hz
5	+140 kg, 0–14 s	—	—	0 (7) stop hits, lowest x −76.4 mm, twin settles −54.9 mm
5	leveling off, or $h_{SP} = +20$ mm	—	—	3 stop hits, or peak compression 56.4 mm
6	60 % worn, first hump, 0–10 s	peak 3.83 (5.90), 1.234 (1.197) rms	—	±13.9 (±2.0) mm 1.6–2.4 s after the hump
6	bounce test, level road	—	—	62.2 to 32.9 mm (51.8 to 9.9 mm) in one cycle
7	0 %, 2.5–4 s	—	24.0 (43.6) %	request peak 1438 N
7	derated to 500 N, 4.5–9 s	2.93 (2.62) rms	75.2 (43.6) %	clipped 92.1 % of the time, 54 liftoffs
7	derating removed at 9 s, 10–15 s	—	24.1 %	no liftoff
8	clean preview, 2–8 s	0.76, off 0.90 (1.09) rms	—	—
8	25 mm noise, 9–20 s	1.22, off 1.01 (1.23) rms	—	window 1 m 0.87, gain 0.5 1.00
10	100 %, no preview	−35.9 % against twin	—	6 liftoffs, 0 stop hits, 72 J
10	80 %, no preview	−17.4 %	—	no liftoff
10	80 % with preview	−28.5 %	—	no liftoff, 0 stop hits, 191 J

its plant-specific model, observer and weights. It applies only to the active strut. Its model uses travel $x = z_s - z_u$, velocities v_s, v_u, wheel height relative to road $\eta = z_u - z_r$, actuator force f and a body-force disturbance d. Force variables f, d, u are in kN, and the nominal contact-mode balances are

$$\begin{aligned} \dot{x} &= v_s - v_u, & \dot{\eta} &= v_u - v_r, \\ M_s \dot{v}_s &= -k_s x - c(v_s - v_u) + 10^3 (f + d), & & \\ m_u \dot{v}_u &= k_s x + c(v_s - v_u) - k_t \eta & & \\ &\quad - c_t (v_u - v_r) - 10^3 f, & & \\ \tau_a \dot{f} &= u - f, & \dot{d} &= 0. \end{aligned} \tag{11.14}$$

The declared values are $M_s = 360\,\text{kg}$, $m_u = 40\,\text{kg}$, $k_s = 25\,\text{kN/m}$, $k_t = 200\,\text{kN/m}$, $c = 500\,\text{N s/m}$, $c_t = 100\,\text{N s/m}$ and $\tau_a = 10\,\text{ms}$. These remain fixed when load, stiffness or actuator lag changes. Flight and stops are absent from prediction. Against the original nominal plant derivatives at two signed contact states, the matrix calculation agrees within 2.2×10^{-14}.

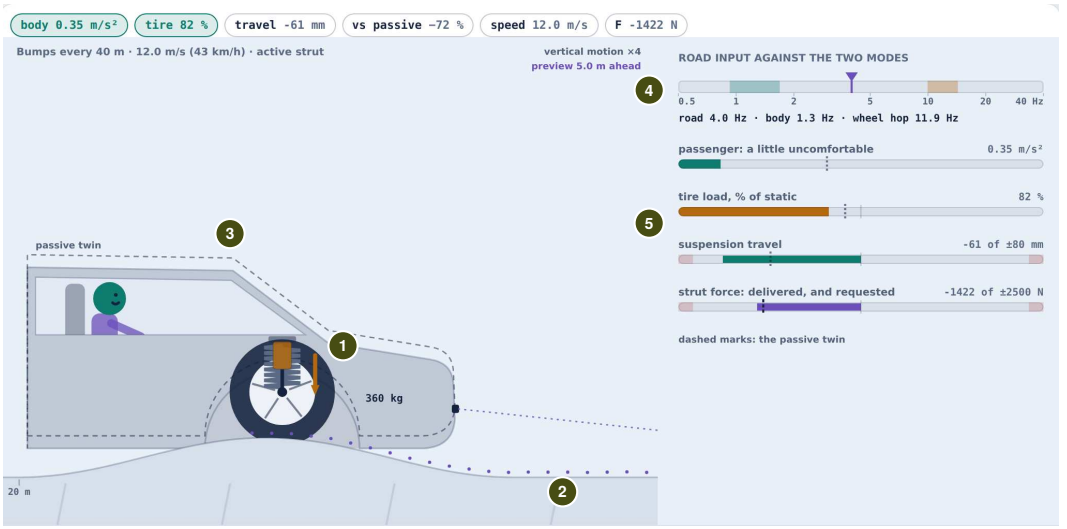


Figure 11.3 Case 1, the isolated hump, with road preview on, paused in automatic mode at $t = 1.80$ s. The picture is the plant view of the screen. The wheel is 1.6 m into the first 60 mm hump. In the cutaway the actuator arrow (1) points down as the strut retracts, a row of dots (2) marks the preview readings of the road ahead, and the dashed outline of the passive twin (3) rides above the active body. Beside it the road input at 4.0 Hz lies between the body band at 1.3 Hz and the wheel-hop band at 11.9 Hz (4), and the bars (5) read a running comfort of 0.35 m/s^2, a tire load of 82 %, 61 mm of the 80 mm compression travel and a delivered strut force of −1422 N, with the request marked beside it.

A six-state steady-state Kalman gain is applied to the existing delayed body/wheel accelerometers and raw height sensor. The observer corrects the preceding nominal 2 ms state before propagating, accounting for one report-delay step. Its discrete process covariance diagonal is $[10^{-9}, 10^{-5}, 10^{-9}, 10^{-4}, 10^{-6}, 10^{-7}]$ in the stated state units, and measurement covariance is $[0.02^2, 0.2^2, 0.0005^2]$. The covariance iteration converges in 528 steps to relative change 9.98×10^{-12}. The disturbance state is bounded at ± 5 kN and provides constant-force offset correction [17], without identifying passenger mass. On the new case the travel and tire-deflection estimation RMS are 0.108 and 0.0587 mm, and actuator-force estimation RMS is 0.183 N. Those values do not characterize flight or noisy-preview operation.

Only slopes interpolated from camera samples already stored at the current decision enter v_r. The controller integrates its own distance from the applied speed. Outside camera support, road height is held. At 12 m/s, the five-meter preview covers about 21 of 25 future intervals, not the entire horizon. Preview Off supplies no road input. Neither true position, physical state, route function, future disturbance nor current physical coefficient enters the new model. Volume 20, Chapter 5 plans a foil's flap in the same way, on water the bow has already measured.

Every 20 ms, a shared quadratic optimizer predicts 25 steps, 0.5 s, in ten move blocks [18]. Outputs are body acceleration, travel in cm and elastic tire-load variation in kN. Tracking weights are $[0.1 + 4w, 0.02, 0.1 + 4(1 - w)]$, with independent MPC comfort $w = 0.7$, terminal travel weight 0.2, force weight 0.002 and move weight 0.02. The ride-height target is retained. Force availability and moves up to the smaller of 400 N and the physical two-millisecond slew allowance are hard. Nominal travel within ±80 mm and elastic load $(M_s + m_u)g - k_t\eta \geq 0$ are soft, each with quadratic price 100 and linear price 1. The elastic surrogate omits tire damping, so it is not an actual contact guarantee. The leveling PI tracks each applied command once. A rejected plan holds force on handover, marks

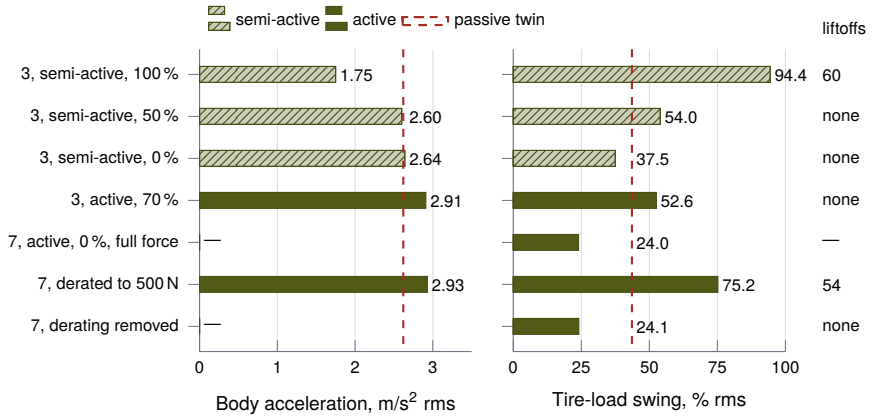


Figure 11.4 The washboard rows of Table 11.4, cases 3 and 7 at 15 m/s, with the passive twin's 2.62 m/s^2 and 43.6 % as dashed lines. Hatched bars are the semi-active strut at the comfort preference named, solid bars the active strut, and a dash marks a value the table does not report. Notice that the one setting that beats the twin's comfort by much is also the one that more than doubles its tire-load swing and leaves the road 60 times.

the historian and returns to the original law until recovery. The first solve primes the run.

11.6 Scenarios and Measured Results

The ten scenarios are listed in Table 11.3 and the measured outcomes in Table 11.4. Scenarios, completion rules and the data export work as Section 1.6.4 describes. All values come from runs of the engine at the scenario's seed with the settings named, changed at $t = 0$ unless a time is given, and windows are simulated time from the start of the run. A setting chosen before Run gives the same run as the same setting carried through Reset. Values over a window, and peaks, are taken at every 0.5 ms physics step. Every scenario starts from the same base settings, the active strut at 70 % comfort with $C_{sky} = 4000\,\mathrm{N\,s/m}$, $C_{gnd} = 2500\,\mathrm{N\,s/m}$, leveling on and preview off, and changes only what Table 11.3 lists. Figure 11.4 draws the washboard rows of Table 11.4, cases 3 and 7, against the passive twin.

> ✦ DID YOU KNOW? **A Worn Damper Feels Softer**
>
> From the simulator: on the first hump a damper that has lost 60 % of its damping peaks at 3.83 m/s^2 against 5.90 m/s^2 for the twin, and over 10 s it reads 1.234 m/s^2 rms against 1.197 m/s^2 (Table 11.4). The comfort number barely moves while the body still swings ±13.9 mm against ±2.0 mm after the hump.

11.6.1 Comfort, Grip and Work With a Finite Preview

Case 9 compares the two active laws with preview On over 8 s, seed 20261013 (Figure 11.5). MPC body acceleration RMS is 0.1550 versus 0.3148 m/s^2, and peak travel 55.4 versus 61.1 mm. Tire-load RMS is 3.78 versus 3.89% of static, with no liftoff or stop under either. Positive mechanical work increases to 148.2 from 92.4 J. A six-point hindsight grid includes a classical 100% comfort, $C_{sky} = 5000\,\mathrm{N\,s/m}$ setting with still lower RMS 0.1352 m/s^2 and 139.2 J, at more travel 63.6 mm. Thus the nominal MPC is not uniformly superior. Replacing only the original velocity estimates with Kalman estimates gives RMS 0.3281 m/s^2, so the main improvement is not explained by that estimator substitution alone. Both laws use the same camera buffer, and no additional route preview is supplied.

Table 11.5 Matched Active-Law Runs, Original / MPC

Case	Body RMS	Travel mm	Lifts	Work J
New, 8 s	.315 / .155	61.1 / 55.4	0 / 0	92 / 148
No preview, 8 s	.808 / .957	46.8 / 44.3	0 / 0	1 / 15
Pothole, 8 s	1.182 / 1.001	57.9 / 65.0	4 / 6	12 / 158
Load, 8 s	.667 / .511	76.4 / 78.5	0 / 0	89 / 162
Noisy, 20 s	1.042 / 2.184	38.4 / 85.9	0 / 4	481 / 1888
Suggested route	.885 / .653	66.7 / 65.4	0 / 5	191 / 369

RMS in m/s^2. MPC plans/mean Node microseconds: new 400/130, pothole 400/66, load 400/50, noisy 1000/80, route 617/68. No rejected plans in these runs.

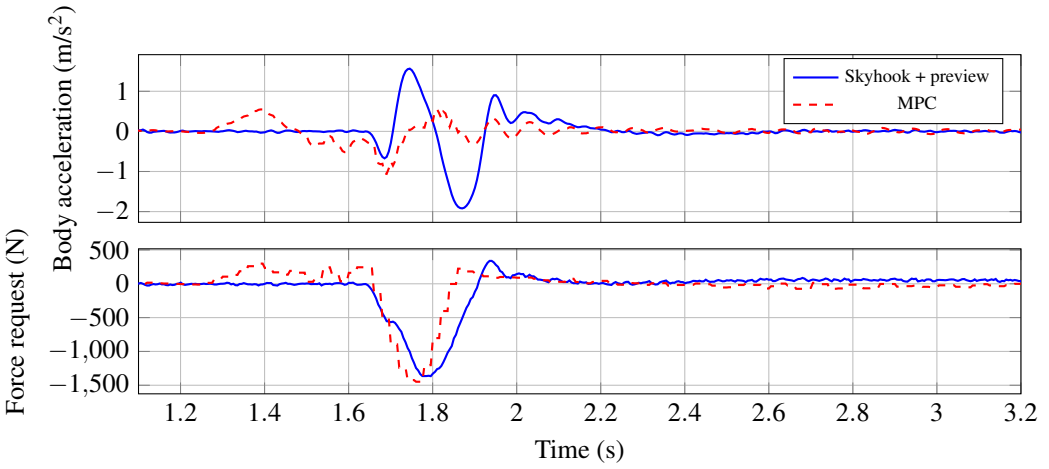


Figure 11.5 The first hump of case 9 under the same road camera, skyhook with preview as solid lines and the MPC as dashed lines. The force plan reduces body acceleration, while its greater positive mechanical work and its losses on contact-limited cases remain separate outcomes.

Without preview, MPC loses on the bump, RMS 0.9566 versus 0.8077 m/s^2. On a pothole it lowers RMS but raises tire-load variation and liftoffs from four to six. On the suggested route it lowers RMS to 0.6534 from 0.8854 m/s^2, but five liftoffs make it fail while the original suggested law passes. With a 0.3 m smoothing window in the noisy-preview case, MPC RMS is 2.184 versus 1.042 m/s^2, with four liftoffs and one stop versus none. A 1 m window improves MPC RMS to 0.6131 versus 0.8027 m/s^2, but tire-load variation is 20.99 versus 15.71% and work 682 versus 244.5 J. Modeled contact and soft bands do not preserve grip when the forecast is wrong.

The measurements behind this comparison fill 36 rows. They include passive and semi-active alternatives, active hardware on the washboard, six hindsight settings and half-step runs. The semi-active washboard results are identical under both laws because the MPC is inactive on that hardware. Halving the physics step retains the new-case ordering. Table 11.5 reports the separate objectives and planner workload. An unconstrained one-step instance of this actual nominal model agrees exactly with its hand normal equation.

Timing 125 plans in the browser per viewport gives mean solve times of 0.397 to 0.704 ms across six viewport and theme runs. At real-time playback the planner occupies 1.98 to 3.52 % of a CPU core, and twice that at the top two-times speed. Observer and rendering costs are excluded.

11.6.2 A Hump, With and Without the Road Ahead

Case 1 crosses a hump 60 mm high and 3 m long every 40 m at 12 m/s, the road input arriving at 4.0 Hz. Over the first hump the passive twin's body rises 47.7 mm, swings 20.8 mm below level on

the rebound and peaks at 5.90 m/s^2. The active strut at 70 % comfort rises 36.7 mm, undershoots 5.3 mm and peaks at 4.72 m/s^2, and 1.5 s after the wheel meets the hump the active body is 0.2 mm from level while the twin is still 3.7 mm below. At 100 % comfort the rise is 28.4 mm and the peak 3.09 m/s^2. The skyhook term pushes against the body's own velocity rather than against the relative velocity a damper sees, so it damps the rebound without passing the road's velocity to the body, and the body is still carried over the hump by the spring.

Preview changes the order of events. The strut starts retracting before the wheel reaches the hump, absorbs 61.1 mm of travel itself, and the body rises only 5.9 mm with a peak of 1.92 m/s^2 (Table 11.4), and Figure 11.3 shows the strut retracting over the hump. Over the first 10 s, which include three humps, the body acceleration is 0.885 m/s^2 rms against 1.197 m/s^2 for the twin, and 0.345 m/s^2 with preview. The price is actuator work, 138 J with preview against 1 J without, because the actuator now does the work of compressing the spring over each hump, where without preview it mostly absorbs power.

11.6.3 A Pothole No Strut Can Follow

Case 2 meets a pothole 50 mm deep and 0.9 m long with 0.15 m edges at 12 m/s, where the entry edge asks for 1579 m/s^2 of downward wheel acceleration and the wheel has 98.1 m/s^2. Dropping in is gentle for the body because the tire simply leaves the road, once for 29.0 ms on the twin and twice for 42.0 ms in all on the active strut. The jolt comes on the far side, where the falling wheel meets the rising road 0.15 m past the edge for the twin and 0.22 m past it for the active strut, at 13.65 m/s^2 and 11.45 m/s^2. Moving the preference to road holding barely helps, with one flight of 27.5 ms at 0 % comfort, because no damping law pulls the wheel down faster than its spring does. Preview presses the tire down just before the edge and cuts the flight to 32.0 ms and the peak to 9.73 m/s^2. Slowing to 3 m/s, where the edge asks for 98.7 m/s^2, still leaves the active strut airborne for 12.0 ms and the twin for 19.5 ms, and only with preview does the tire stay down, consistent with the 2.99 m/s and 3.83 m/s limits of Section 11.4.

11.6.4 Wheel Hop Found by Tuning and by Speed

Case 3 drives the washboard at 15 m/s, 12.0 Hz against the 11.9 Hz wheel hop, on the semi-active strut at 100 % comfort. From 3 to 8 s the body acceleration is 1.75 m/s^2 rms against 2.62 m/s^2 for the twin, a third lower, while the tire-load swing is 94.4 % against 43.6 % and the wheel leaves the road 60 times, once per ripple, for 1.62 s of the 5 s. The skyhook request is small at 12 Hz, so the valve never rises above 840 N s/m and the wheel is damped by little more than c_{min}, which is the soft curve of Figure 11.2 crossing the liftoff line. At 50 % the swing falls to 54.0 % with the tire load never below 898 N, and at 0 % to 37.5 %, better than the twin, with the body at 2.64 m/s^2, level with the twin as the nearby invariant point of Equation (11.9) leads one to expect. Only the setting that let the wheel fly moved the body acceleration by more than 1 %. The default active strut does worse than the passive twin on both measures here, 2.91 m/s^2 and 52.6 %. This is likely because its instantaneous damping is only the 500 N s/m residual damper, while the controller's force arrives through a lag and a delay that alone cost 46° at wheel hop.

> **TRY IT IN THE APP** **3 · Washboard Road**
>
> Load the scenario, press Run and watch the wheel and the red paint it leaves on the road. Set for comfort, the semi-active strut holds the body acceleration to 1.75 m/s^2 rms against 2.62 m/s^2 for the passive twin, a third lower. From 3 to 8 s the wheel pays for it: it leaves the road 60 times, airborne for 1.62 s of the 5 s.

Case 4 reaches the same band with speed alone. The passive car on the washboard sees 0.92 m/s^2 rms and a 8.6 % swing at 6 m/s once the ripples are fully under the wheel, and 2.62 m/s^2 and 43.6 % after the step to 15 m/s. A shipped test counts the tire load crossing its static value at 12.00 Hz, which is v/λ. At 28 m/s the ripples arrive at 22.4 Hz, above the band, and the ride improves to 1.11 m/s^2

and 32.5 %, because the wheel's own mass now filters the ripples. Worse is not a function of speed but of where the speed puts the road frequency, which Figure 11.2 draws.

11.6.5 Load and the Travel It Takes

Case 5 adds 140 kg to the corner at 0.2 s on the hump road at 10 m/s. The passive twin settles with its ride height 54.9 mm below the design value, which is $\Delta Mg/k_s$, and hits its bump stop 7 times in 14 s, once as the load lands and twice at each of the three humps. The active body plunges to −70.5 mm, is still 32.6 mm low when the first hump arrives at 2.0 s, and is back within 5 mm of its setpoint 5.1 s after the step. It never touches the stop, coming within 3.6 mm of it at −76.4 mm on the first hump, because the leveling force already carries most of the new weight and the skyhook term resists the rest of the plunge. At the end of the run the leveling loop holds 1373 N, which is 140 kg times g and 55 % of the actuator rating, authority the comfort terms no longer have. With the leveling off the active strut hits the stop 3 times. Raising the setpoint to +20 mm before the run starts the car 20 mm higher and keeps the peak compression to 56.4 mm, 20 mm less than at the design setpoint.

11.6.6 A Worn Damper and a Derated Actuator

Case 6 runs the hump road on a passive damper that has lost 60 % of its damping. The first hump feels softer, 3.83 m/s^2 against 5.90 m/s^2 for the healthy twin, because a weak damper passes less of the wheel's sudden motion to the body. The cost comes afterward. From 1.6 to 2.4 s after the wheel meets the hump the worn body still swings ±13.9 mm against ±2.0 mm, yet the body acceleration over 10 s, 1.234 m/s^2 against 1.197 m/s^2, barely records the fault. In the bounce test on level road the healthy damper cuts the bounce from 51.8 to 9.9 mm in one cycle and the worn one only from 62.2 to 32.9 mm, and on the washboard at 15 m/s the worn damper lets the wheel leave the road 60 times in 5 s. The active strut is unaffected by wear, and in the same push test its body stops at −43.0 mm and rebounds 10.8 mm.

Case 7 runs the active strut at 0 % comfort on the washboard. From 2.5 to 4 s the groundhook requests peak at 1438 N and hold the tire-load swing to 24.0 % against 43.6 % for the twin. At 4 s a thermal derating cuts the available force to 500 N. From 4.5 to 9 s the request is clipped 92.1 % of the time, the swing rises to 75.2 %, the body to 2.93 m/s^2 against 2.62 m/s^2, and the wheel leaves the road 54 times. A clipped force damps the wheel less the larger its motion becomes, so the hop grows until the tire leaves the road. With the derating removed at 9 s the swing returns to 24.1 % with no liftoff.

> **TRY IT IN THE APP** **7 · Actuator Saturation**
>
> Press Run and watch the force and Tire load strips. At 4 s the actuator is derated to 500 N. From 4.5 to 9 s the request is clipped 92.1 % of the time, the tire-load swing rises from 24.0 to 75.2 % rms and the wheel leaves the road 54 times. Set Actuator derating back to 0 % near 9 s, and the swing returns to 24.1 %.

11.6.7 Preview Through Spray

Case 8 drives rough asphalt at 15 m/s with preview on. From 2 to 8 s, with a clean reading, the body acceleration is 0.76 m/s^2 rms against 0.90 m/s^2 with preview off and 1.09 m/s^2 for the twin. At 8 s the reading turns noisy, 25 mm on a road that varies by a few millimeters, and from 9 to 20 s the noisy preview gives 1.22 m/s^2, as bad as the twin's 1.23 m/s^2, against 1.01 m/s^2 with preview switched off. The slope fitted to a noisy reading is mostly noise, and the preview force grows from 242 N rms on the clean reading to 740 N. Widening the smoothing window from 0.3 to 1 m averages the noise and keeps the longer road features, cuts the preview force to 290 N and brings the body to 0.87 m/s^2, while halving the preview gain reaches only 1.00 m/s^2. The 1 m window is also slightly better on the clean reading, 0.74 m/s^2 against 0.76 m/s^2.

11.6.8 The Graded Route

The challenge drives the 185 m route at 15 m/s and asks for a body acceleration at least 25 % below the twin's with no liftoff and no bump-stop contact. The verdict is taken when the route ends, and it counts only if the speed stays at 15 m/s and the load at 60 kg throughout and no model parameter or disturbance is changed. At 10 m/s the shipped tune would meet the comfort, liftoff and stop criteria at −47.1 %, which is why the speed is part of the case. Reset keeps the learner's setting and redraws the same seeded road, so each retry drives the same route. The twin finishes in 12.33 s at 1.238 m/s^2 rms, so the target is 0.928 m/s^2. As shipped, at 100 % comfort without preview, the body is 35.9 % better than the twin and the wheel leaves the road 6 times on the washboard, which fails the target. Moving to 80 % stops the liftoffs and leaves only 17.4 %. With preview at 80 % the body is 28.5 % better, a margin of 3.5 percentage points over the target, with no liftoff and no stop contact, for 191 J of actuator work against 72 J as shipped. A sweep in steps of 5 % passes at 75, 80 and 85 % with preview and at no setting without it. Without preview the only setting that reaches −25 %, 90 % at −25.1 %, leaves the road 5 times. At 0 % the body acceleration more than doubles, 104.0 % above the twin's, with one stop contact on the final hump, while on the rough section the body swings at about 1.16 Hz, the lightly damped body mode of Section 11.5.

11.7 Technology in Practice

What Measures It

Like the controller of this chapter, a production semi-active corner reads two accelerometers or an accelerometer and a stroke sensor [5]. The chapter's leaky integrators rebuild both velocities from the accelerations, and their leak hides motion slower than about 0.16 Hz. The road ahead can be scanned directly by a lidar, which costs much, or reconstructed from camera images as a height map [19]. The chapter's preview sensor stands for either and reads the road 5 m ahead with independent noise.

> **TECHNOLOGY** **Sensor: Accelerometers on the Body and the Wheel**
>
> A semi-active corner is usually read by two sensors per axle, either two accelerometers or an accelerometer and a stroke sensor that measures the suspension travel. Sensors weigh heavily on the cost, so the trend is toward one sensor per corner, with the second signal reconstructed by filtering, and toward sharing the sensors with stability and rollover control [5]. On one test car with semi-active dampers a prototype control unit read three vertical accelerometers on the body and two on the wheels [20]. The chapter's corner carries both accelerometers and the ride-height sensor.

What Moves It

The semi-active strut moves nothing itself: its valve only sets how hard the damper resists. The active strut must supply force. Hydraulic actuators are durable, deliver high forces and withstand high impulses, but they are complex to model, and in a heavy machine's hydraulic driveline the delay between a command and the actuator's response is large and depends on what the other actuators are doing [21]. The chapter's actuator is a first-order lag of 10 ms with a force limit of 2500 N and a slew limit of 400 kN/s.

> **TECHNOLOGY** **Final Element: A Damper Whose Valve Sets Its Force**
>
> Most semi-active dampers use solenoid valves in an electro-hydraulic circuit, and magnetorheological and electrorheological ones were expected to grow [5]. In a magnetorheological damper, micron-scale ferrous particles in a carrier fluid form chains under a magnetic field and raise its yield stress, and the damper can switch from near-minimal to high damping within milliseconds [22]. A real damper's force is not one coefficient times the stroke velocity: it lies in a region between a minimum and a maximum force curve, each a nonlinear function of that velocity, and the command interpolates between them [20]. The chapter's damper is linear, 300 to 4500 N s/m, behind a 15 ms valve lag.

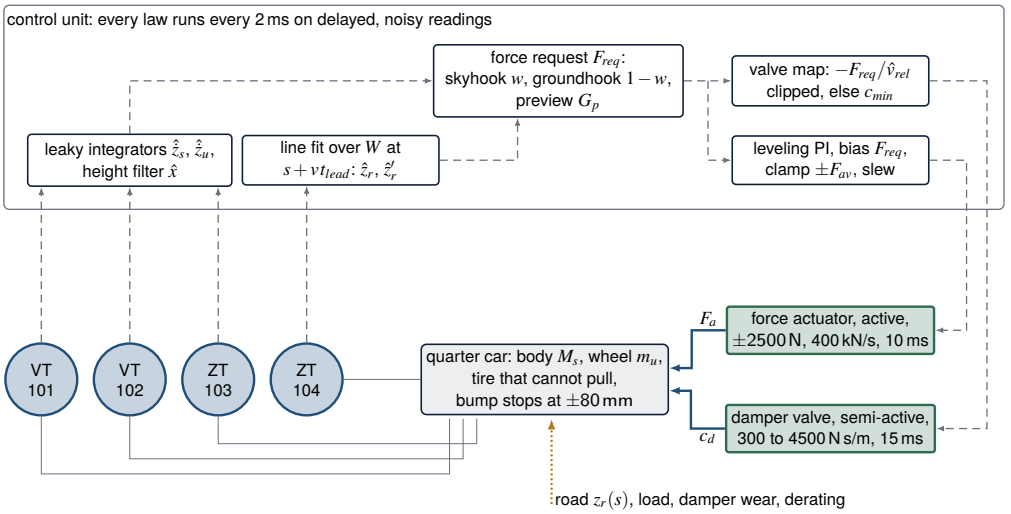


Figure 11.6 The suspension loop on vehicle hardware. The accelerometers VT-101 and VT-102 and the ride-height sensor ZT-103 feed the estimates, and the preview sensor ZT-104 feeds a line fit of the road the wheel is about to meet. One force request serves both struts: on the semi-active strut the valve map turns it into a damping coefficient, and on the active strut it enters the leveling PI as its bias before the clamp and the slew limit. Notice that the same request reaches two very different final elements, and that only the actuator can deliver a force with the sign that feeds energy in.

Where the Controller Runs

On one test car with semi-active dampers the control software ran on a prototype electronic control unit that sent a target current to each damper. Its parameters could be changed while driving from a laptop on the vehicle's network, and a commercial controller of this kind may hold hundreds of tunable parameters [20]. The chapter's controller runs every 2 ms, a 500 Hz loop. Its structure is one force request, the sum of the skyhook, groundhook and preview terms, which the semi-active valve map turns into a damping coefficient and which the active strut's leveling PI takes as its bias before the clamp and the slew limit. Figure 11.6 draws the loop on that hardware.

> **IN PRACTICE** **Tuning a Semi-Active Suspension on the Road**
>
> Fine-tuning a semi-active suspension is costly. It needs a calibration engineer who understands the control software and a professional driver who judges each proposed calibration, many hours of driving, and on a production vehicle it may take months. Most makers rely on the driver's subjective evaluation, and the comfort index of ISO 2631-1 is seldom used for suspensions in industry. Indoor alternatives place the driver in a hardware-in-the-loop simulator whose road is emulated by a robotic arm, or the car on four moving platforms. Each test on the road follows the same segment at the same speed profile, so that the road excites the same frequencies [20].

What Is Modernizing It

Three developments are changing the hardware around this loop. Road reconstruction from a top-down view of camera images reached elevation errors of 1.83 cm with one camera and 0.50 cm with a stereo pair on a real-world data set, which its authors judge promising for practical road preview [19]. Data-driven calibration with Bayesian optimization tuned a production car's semi-active controller in about an hour of experiments, where tuning by hand may take months [20]. Learned controllers for

active suspensions have moved from simulation to a real hydraulic machine, and they transferred well only when trained with actuator delays and a penalty on erratic actions [21]. The predictive force law of Section 11.5.7 is a fourth path, and its failures on the route and under a noisy camera show what a wrong forecast costs.

11.8 Limitations

The model is one corner in vertical motion. Without pitch, roll, load transfer or a seat, it has nothing to say about the heave, pitch and roll control that production active systems perform.

The tire is a point contact with a linear spring and a light damper. It does not envelop short features or bridge ripples, and grip is represented by the vertical load alone rather than by longitudinal and lateral forces. Chapter 4 models the longitudinal force against wheel slip that this chapter leaves out.

> **OPEN CHALLENGE** **Semi-Active Control Beyond Steady Driving**
>
> The bulk of semi-active control laws was designed for quasi-steady driving, with no hard acceleration, braking or steering. A semi-active suspension is fully exploited only when every working condition is considered, and much current research seeks the best handling of transients, where the damper can assist stability control, traction control and anti-lock braking [5]. Braking and cornering bring in pitch, roll and load transfer, which is also where this chapter's single corner breaks down. Progress would be a damper law that keeps the tire load up through braking and cornering as well as on a straight road.

The actuator energy counts positive mechanical work only. A hydraulic unit also spends power holding a static leveling force, so the 1373 N of case 5 costs nothing here.

Comfort is unweighted rms acceleration. It weights every frequency equally while discomfort depends on frequency, and the ISO 2631-1 words on the passenger are indicative only [16].

The preview reading is the true profile plus independent noise. A camera also misreads shadows, water and painted lines, which bias the reading rather than scatter it, and speed and distance are known exactly. The added MPC fixes nominal masses, stiffnesses, damping and report delay, omits flight and stops, and extrapolates no unseen road feature. Its disturbance estimate is not physical identification, and soft nominal contact and travel limits cannot ensure grip.

> **OPEN CHALLENGE** **Switching Without Shaking**
>
> A blended skyhook and groundhook law works well in a narrow frequency band but can pass higher vibration at other frequencies, and switching between its skyhook and groundhook phases can change the force abruptly and excite high-frequency vibration [22]. Learned controllers show the same trait. A policy rewarded for performance alone switched near its limits like a bang-bang law, which wears equipment, wastes energy and excites higher-order dynamics, and it transferred poorly from simulation to a real hydraulic machine [21]. Progress would be switching laws whose smoothness is designed in and shown on hardware. In the chapter only the valve lag and the actuator's slew limit smooth a switch.

11.9 Conclusion

This chapter studied one force serving two masses on a quarter car with a tire that cannot pull, bump stops, three kinds of strut and a passive twin on the same road. The constraint left when the strut force cancels fixes the body acceleration at 11.25 Hz, just below the 11.9 Hz wheel hop, and the running engine agrees with the linear transfer function to within 0.1 %. Over a 60 mm hump the active strut holds the body rise to 36.7 mm against 47.7 mm, and preview to 5.9 mm. No strut follows a pothole edge at 12 m/s, which asks for 1579 m/s^2 against 98.1 m/s^2 available. On the washboard at wheel hop a semi-active strut set for comfort lowers the body acceleration by a third only by leaving the road 60 times in 5 s, and under the original law on the challenge route only preview with 75 to 85 % comfort meets the target, reaching −28.5 % at 80 %. The leveling loop must stay integral-dominant, since a proportional gain above about 11 N/mm destabilizes the body at 0 % comfort. The model

has one corner, a point tire and unweighted comfort. A fuller model would add pitch and roll, a tire that envelops the road, frequency-weighted comfort and a preview sensor with biased errors. The simulator gives practice in trading competing objectives through a single actuator. The preview MPC adds a measured comfort and travel improvement at greater work, while its route and noisy-camera failures expose the limits of a contact-mode forecast.

KEY POINTS

- The strut pushes the body up and the wheel down with the same force, so it chooses only how the tire's force is shared between them.
- Just below wheel hop the body acceleration is fixed whatever the strut does, and a semi-active strut set for comfort lowers it by a third only by leaving the road 60 times in 5 s.
- A semi-active damper can only dissipate: when the request would feed energy in, its valve goes soft and the delivered force parts from the request.
- Clipped to 500 N, the road-holding force damps the wheel less the larger its motion grows, until the tire leaves the road.

Where else this applies. Volume 17, Chapter 5 sets a plain damper against reactive control, whose power flows both ways, on a heaving buoy, the same line that separates the semi-active strut here from the active one, and its predictive controller acts on a forecast of the waves as preview acts on the road.

References

[1] R. S. Sharp and S. A. Hassan, "The Relative Performance Capabilities of Passive, Active and Semi-Active Car Suspension Systems," *Proceedings of the Institution of Mechanical Engineers, Part D: Transport Engineering*, vol. 200, no. 3, pp. 219–228, 1986.

[2] R. S. Sharp and D. A. Crolla, "Road Vehicle Suspension System Design - a review," *Vehicle System Dynamics*, vol. 16, no. 3, pp. 167–192, 1987.

[3] J. K. Hedrick and T. Butsuen, "Invariant Properties of Automotive Suspensions," *Proceedings of the Institution of Mechanical Engineers, Part D: Journal of Automobile Engineering*, vol. 204, no. 1, pp. 21–27, 1990.

[4] D. Karnopp, M. J. Crosby, and R. A. Harwood, "Vibration Control Using Semi-Active Force Generators," *Journal of Engineering for Industry*, vol. 96, no. 2, pp. 619–626, 1974.

[5] C. Poussot-Vassal, C. Spelta, O. Sename, S. M. Savaresi, and L. Dugard, "Survey and performance evaluation on some automotive semi-active suspension control methods: A comparative study on a single-corner model," *Annual Reviews in Control*, vol. 36, no. 1, pp. 148–160, 2012.

[6] E. K. Bender, "Optimum Linear Preview Control With Application to Vehicle Suspension," *Journal of Basic Engineering*, vol. 90, no. 2, pp. 213–221, 1968.

[7] C. J. Dodds and J. D. Robson, "The description of road surface roughness," *Journal of Sound and Vibration*, vol. 31, no. 2, pp. 175–183, 1973.

[8] M. Tomizuka, "'Optimum Linear Preview Control With Application to Vehicle Suspension'—Revisited," *Journal of Dynamic Systems, Measurement, and Control*, vol. 98, no. 3, pp. 309–315, 1976.

[9] A. G. Thompson, "An Active Suspension with Optimal Linear State Feedback," *Vehicle System Dynamics*, vol. 5, no. 4, pp. 187–203, 1976.

[10] D. Karnopp, "Theoretical Limitations in Active Vehicle Suspensions," *Vehicle System Dynamics*, vol. 15, no. 1, pp. 41–54, 1986.

[11] M. Valášek, M. Novák, Z. Šika, and O. Vaculín, "Extended Ground-Hook - New Concept of Semi-Active Control of Truck's Suspension," *Vehicle System Dynamics*, vol. 27, no. 5–6, pp. 289–303, 1997.

[12] J. D. Carlson and M. R. Jolly, "MR fluid, foam and elastomer devices," *Mechatronics*, vol. 10, no. 4–5, pp. 555–569, 2000.

[13] D. Hrovat, "Survey of Advanced Suspension Developments and Related Optimal Control Applications," *Automatica*, vol. 33, no. 10, pp. 1781–1817, 1997.

[14] C. Gohrle, A. Schindler, A. Wagner, and O. Sawodny, "Design and Vehicle Implementation of Preview Active Suspension Controllers," *IEEE Transactions on Control Systems Technology*, vol. 22, no. 3, pp. 1135–1142, 2014.

[15] H. E. Tseng and D. Hrovat, "State of the art survey: active and semi-active suspension control," *Vehicle System Dynamics*, vol. 53, no. 7, pp. 1034–1062, 2015.

[16] M. J. Griffin, "Discomfort from feeling vehicle vibration," *Vehicle System Dynamics*, vol. 45, no. 7–8, pp. 679–698, 2007.

[17] G. Pannocchia and J. B. Rawlings, "Disturbance models for offset-free model-predictive control," *AIChE Journal*, vol. 49, no. 2, pp. 426–437, 2003.

[18] S. J. Qin and T. A. Badgwell, "A survey of industrial model predictive control technology," *Control Engineering Practice*, vol. 11, no. 7, pp. 733–764, 2003.

[19] T. Zhao, L. Yang, Y. Xie, M. Ding, M. Tomizuka, and Y. Wei, "RoadBEV: Road surface reconstruction in bird's eye view," *IEEE Transactions on Intelligent Transportation Systems*, vol. 25, no. 11, pp. 19 088–19 099, 2024.

[20] G. Savaia, Y. Sohn, S. Formentin, G. Panzani, M. Corno, and S. M. Savaresi, "Experimental automatic calibration of a semi-active suspension controller via Bayesian optimization," *Control Engineering Practice*, vol. 112, p. 104826, 2021.

[21] V. Wiberg, E. Wallin, A. Fälldin, T. Semberg, M. Rossander, E. Wadbro, and M. Servin, "Sim-to-real transfer of active suspension control using deep reinforcement learning," *Robotics and Autonomous Systems*, vol. 179, p. 104731, 2024.

[22] H. Lim, J. W. Lee, S.-B. Choi, and J. B. Choi, "VISKY: Virtual inertia skyhook control for semi-active suspension systems using magnetorheological dampers," arXiv:2503.12891v2 [eess.SY], 2025.

11.10 Exercises

11.1 Concept check · 2 min

The road is a sinusoid at $\omega_1 = \sqrt{k_t/m_u}$, about 11.25 Hz for the default car, and the tire stays on the road. Neglect the tire damping. What can the strut force do to the body acceleration there?

(a) Drive it toward zero with a large enough skyhook gain, since the skyhook term acts on the body alone

(b) Nothing: it is fixed at $k_t Z_r/M_s$ whatever the strut does, so only losing tire contact moves it

(c) Halve it, because at ω_1 the travel is fixed at 1.11 times the road amplitude and the strut absorbs the rest

(d) Change it only through the tire load, which at ω_1 is fixed whatever the strut does

11.2 Concept check · 1 min

The semi-active strut receives a request F_{req} with the same sign as the estimated relative velocity $\hat{v}_{rel}$, so $F_{req}\hat{v}_{rel} > 0$. What does its valve do?

(a) It goes to c_{max}, so that the damper delivers as much of the request as it can

(b) It reverses the damper force for one scan, and the residual damper absorbs the difference

(c) It goes to c_{min}, and the delivered force parts from the requested one on the force trend

(d) It holds the previous valve setting until the sign of the request changes again

11.3 Concept check · 2 min

The load-leveling loop of the active strut runs at $K_c = 5\,\mathrm{N/mm}$ and $\tau_I = 0.5\,\mathrm{s}$, an integral-dominant tuning. Why is the proportional gain kept this small?

(a) A larger K_c would leave a ride-height offset under the extra load that the integral could not remove

(b) A larger K_c would amplify the 0.5 mm ride-height noise enough to saturate the actuator

(c) A larger K_c would excite wheel hop at 11.9 Hz through the height filter and the strut

(d) Behind the 1 s height filter the proportional term lags nearly 90° at the body mode and adds negative damping

11.4 Theory and calculation · 7 min

Use the default car of Table 11.2: $m_s = 300\,\mathrm{kg}$ with the 60 kg design load aboard, $m_u = 40\,\mathrm{kg}$, $k_s = 25\,\mathrm{kN/m}$ and $k_t = 200\,\mathrm{kN/m}$. Neglect all damping.

(a) Find M_s and the body and wheel-hop frequencies from the approximations of Section 11.4. *Checkpoint:* 360 kg, 1.25 Hz and 11.94 Hz.

(b) Find the first invariant frequency $\omega_1/2\pi$ and the body acceleration per millimeter of road there. What amplitude and rms does the 7 mm washboard give at that frequency, whatever the strut? *Checkpoint:* 11.25 Hz, 0.556 m/s^2 per mm, 3.89 m/s^2 amplitude and 2.75 m/s^2 rms.

(c) Find $\omega_2/2\pi$ and the travel per millimeter of road there. At what speeds does the 1.25 m washboard reach ω_1 and wheel hop? *Checkpoint:* 3.56 Hz, 1.11, 14.1 m/s and 14.9 m/s.

11.5 Theory and calculation · 6 min

Case 2 meets a pothole of depth $D = 50$ mm whose entry edge is a half-cosine of length $e = 0.15$ m, Equation (11.5). Use $g = 9.81\,\mathrm{m/s^2}$ and the default car.

(a) Find the largest downward wheel acceleration the edge asks for, $(D/2)(\pi v/e)^2$, at 12 and 3 m/s. *Checkpoint:* 1579 m/s^2 and 98.7 m/s^2.

(b) Once the tire unloads, find the downward acceleration the spring preload and the wheel's weight give, $(F_{s0} + m_u g)/m_u$, and the value with the full 2500 N actuator pushing the wheel down as well. *Checkpoint:* 98.1 m/s^2 and 160.6 m/s^2.

(c) Find the highest speed at which the wheel can follow the edge in each case. *Checkpoint:* 2.99 m/s and 3.83 m/s.

11.6 Theory and calculation · 7 min

An engineer checks the timing of the active strut against the defaults of Table 11.2. Take $\omega_b = 2\pi(1.25\,\mathrm{Hz})$ and wheel hop at 11.94 Hz.

(a) The 1 s height filter turns the leveling gain into a negative damping of about $K_c/(\omega_b^2 \tau_h)$. Find it at 5 and 50 N/mm and compare it with the 500 N s/m residual damper. *Checkpoint:* 81 N s/m and 811 N s/m.

(b) Find the highest frequency at which a full 2500 N sinusoid can be followed under the 400 kN/s slew limit, and under 50 kN/s. *Checkpoint:* 25.5 Hz and 3.18 Hz.

(c) Find the phase the 10 ms actuator lag and the 2 ms sensor delay together cost at wheel hop. *Checkpoint:* 36.9° plus 8.6°, about 46°.

11.7 App challenge · 8 min

Open case 1, "1 · Isolated bump", at the default seed and the default 0.5× speed (a 10 s run takes 20 s).

(a) Run as shipped and pause when the Ride time tile reads 10.0 s. Read the Body acceleration rms, Tire load rms and Actuator energy tiles. *Checkpoint:* 0.885 m/s^2 (passive 1.197), 8.1 % (passive 11.0), 1 J, each within 0.005 or one unit of the last digit.

(b) Press Reset, set Road preview to On, and run again to 10.0 s. Read the same tiles and Peak travel. *Checkpoint:* 0.345 m/s^2, 4.3 %, 138 J, 61 of 80 mm.

(c) Explain why the actuator work rises more than a hundredfold while the body acceleration falls by more than half, and why preview uses more travel. *Checkpoint:* The actuator now compresses the strut over each hump.

11.8 App challenge · 8 min

Open case 5, "5 · Heavier passenger load", at the default seed and the default 0.5× speed. The extra 140 kg lands at 0.2 s.

(a) Run as shipped and pause when Ride time reads 12.0 s. Read the Bump-stop hits and Peak travel tiles. Export the CSV and read `ctrl_lev_N` in the row `time_s` = 12.00. *Checkpoint:* 0 (passive 7), 76 of 80 mm, 1370 N within 2 N.

(b) Find the static force that carries 140 kg and its share of the 2500 N rating, and compare with (a). *Checkpoint:* 1373 N, 55 %.

(c) Press Reset and, before pressing Run, set Leveling gain to 0 and Leveling integral time to 20 s. Run to 12.0 s and read the same two tiles. *Checkpoint:* 3 (passive 7), 89 of 80 mm.

11.9 App challenge · 9 min

Open the challenge, "Challenge · three surfaces", at the default seed and the default 0.5× speed. Each run stops itself 0.5 s after the route ends, at 12.8 s of simulated time.

(a) Run as shipped. Read Comfort vs passive, Wheel off the road and Challenge target. *Checkpoint:* −35.9 %, 0.122 s and 6 times, not met.

(b) Set Comfort ↔ road holding to 80 %, press Reset and run the route again. Read the same tiles. *Checkpoint:* −17.4 %, no liftoff, not met.

(c) Set Road preview to On, press Reset and run once more. Read the same tiles and Actuator energy, and say why preview is what makes the setting pass. *Checkpoint:* −28.5 %, no liftoff, met, 191 J.

11.10 Application area · 4 min

A worn passive damper has lost 60 % of its damping. In case 6 the first hump peaks at 3.83 m/s^2 against 5.90 m/s^2 for the healthy twin, and the body acceleration over 10 s is 1.234 m/s^2 against 1.197 m/s^2. In the bounce test the healthy body falls from 51.8 to 9.9 mm in one cycle and the worn one from 62.2 to 32.9 mm.

(a) From the bounce test, find the ratio of successive peaks and the damping ratio $\zeta = \delta/\sqrt{4\pi^2+\delta^2}$ with $\delta = \ln(x_1/x_2)$ for each damper. *Checkpoint:* 0.19 and 0.53, ζ 0.25 and 0.10.

(b) Why would a driver or a comfort rating fail to flag this damper, and which measurement would? *Checkpoint:* The comfort number moves by 3 %. Measure the decay or the lowest tire load.

11.11 Application area · 3 min

A production car reads the road ahead with a camera. In case 8 a clean reading gives 0.76 m/s^2 rms against 0.90 m/s^2 without preview. After spray makes the reading noisy the preview gives 1.22 m/s^2, as bad as the passive twin, against 1.01 m/s^2 with preview off, and the preview force rises from 242 N to 740 N rms.

(a) What should a supervisor do when the reading degrades, and which signal available to the controller could tell it so without knowing the true road? *Checkpoint:* Fall back to feedback or smooth more. Watch the preview force.

(b) Which camera error does the simulator leave out, and why would a wider smoothing window not cure it? *Checkpoint:* Biased misreadings such as shadows, water and painted lines.

11.12 Review the agent · 5 min

An AI assistant tunes the challenge. It writes: "In case 9 the MPC halves the body acceleration of skyhook with preview, 0.155 m/s^2 against 0.315 m/s^2, with no liftoff. Its model also keeps a band on the tire load. So keep 80 % comfort and preview On, select MPC as the Active law, and the challenge will pass with a far larger margin." Find the flaw, and say how you would check the claim on the simulator.